Light Metals 2014
Edited by: John Grandfield
TMS (The Minerals, Metals & Materials Society), 2014

Light Metals 2014

ALUMINUM REDUCTION TECHNOLOGY

Potline Operations – Equipment

SESSION CHAIR
B.K. Kakkar
Carp, ON, Canada

Light Metals 2014
Edited by: John Grandfield
TMS (The Minerals, Metals & Materials Society), 2014

A NOVEL DESIGN CRITERION FOR ALUMINA FEEDERS IN ALUMINIUM ELECTROLYSIS CELLS

Asbjørn Solheim

SINTEF Materials and Chemistry
P.O. Box 4760 Sluppen, NO-7465 Trondheim, Norway

Keywords: Alumina, bath, dissolution, feeder

Abstract

The theoretical possibility of agglomeration-free alumina feeding in aluminium reduction cells is addressed. The treatment is based on calculated times for dissolution of alumina particles and their terminal velocity in the bath. It was found that the dissolution rate from a few hundred grams of alumina kept in dispersion is sufficient to supply the entire cell. To derive a criterion for dispersion as single particles and avoiding agglomeration, two types of consideration were made; 1) The volume fraction of solid alumina sinking through the bath at a rate corresponding to the consumption must be considerably below unity, or 2) Particles landing on the bath surface must have time to sink away before they are hit by succeeding particles. The two considerations end up with very similar mathematical expressions. Based on the derived criteria, normal point feeding produces agglomerates, while continuous feeding to the same surface area may produce single particles.

Introduction

When alumina is added to the bath in aluminium reduction cells several dissolution paths are possible, as illustrated in Figure 1. In all cases the process starts with formation of a layer of frozen bath around the particle or agglomerate, which has to melt away before the alumina can dissolve. Agglomeration is associated with the transition from γ-Al_2O_3 to α-Al_2O_3, which is catalysed by fluoride [1] and leads to sintering during recrystallization. Since dissolution of single alumina grains is much faster than dissolution of agglomerates or bottom sludge, the left hand branch in Figure 1 represents the preferred situation.

Intuitively, a larger fraction of the added alumina will be dispersed as single grains if the feeding is slow and distributed into a large bath volume or bath surface area. Compared with older feeding methods (side breaking), point feeders add smaller and more frequent doses. This gives more rapid alumina dissolution, due to a larger fraction dissolved as individual particles and also due to formation of smaller agglomerates.

Point feeding of alumina was introduced by Alcoa in the early 1960s [2], and there is no doubt that this invention represented a quantum leap in the aluminium electrolysis technology. The former sludge problem was at least partly eliminated, and point feeders have been a prerequisite for the amperage increase projects carried out in most companies. Modern cells tend to be full-packed of anodes, and the anode-cathode distance is smaller than before. This gives a smaller volume for dissolution of alumina; *e.g.*, the bath volume per kA was reduced from almost 13 l/kA in AP30 to about 7.5 l/kA for AP3X [3].

Presently, the trend of increased amperage in existing potlines is gradually being replaced by a renewed interest in technology for reduced specific energy consumption. This does not make alumina feeding simpler, since low bath volume/amperage ratio will also be necessary to reduce the cell voltage.

The present paper is mainly dealing with the conditions for dissolution of the entire amount of alumina in the form of single particles, *i.e.*, agglomeration-free feeding, which would totally eliminate the formation of bottom sludge and lead to a more predictable relationship between feeding and alumina concentration in the bath. The basic construction of the point feeder has not changed since its inception [2], and it might be possible to come up with innovations in this field.

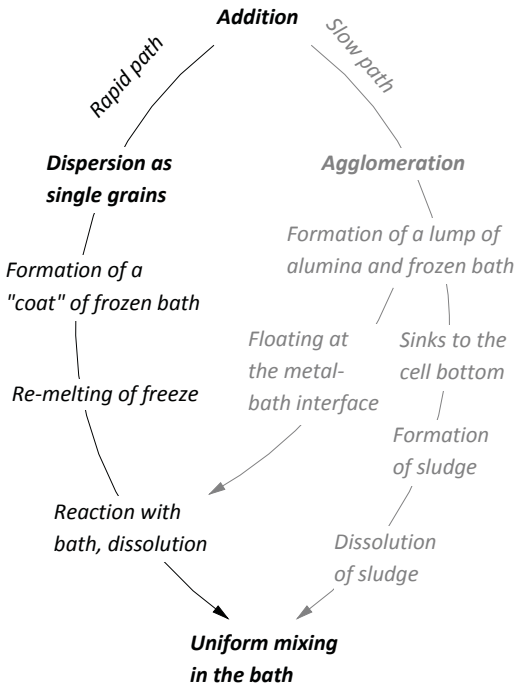

Figure 1. Schematic representation of different paths for dissolution of alumina.

Heat- and Mass Transport Limitations in Alumina Dissolution

Adiabatic Mixing

The dissolution of alumina requires heat, which can be divided into the enthalpy for heating alumina from 298 K to cell temperature, the enthalpy of transition from γ-Al_2O_3 to α-Al_2O_3, and heat of dissolution of α-Al_2O_3. By mixing alumina with bath at adiabatic conditions, this is exactly balanced by the heat associated with cooling of the mixture and freezing of bath.

Figure 2 shows the result of adding γ-Al_2O_3 to a bath with 10 °C superheat at adiabatic conditions. The bath was assumed to contain cryolite, 5 wt% CaF_2, 11 wt% excess AlF_3, and variable amounts of Al_2O_3. The calculation was made using thermodynamic data from JANAF [4], heat of mixing from Solheim and Sterten [5], and phase diagram data from Solheim *et al*. [6] and Skybakmoen *et al*. [7].

As can be observed, only about 1.8 weight percent alumina can be added without causing freezing of the bath. If more alumina is added, the temperature follows the liquidus temperature for crystallisation of cryolite until the cryolite-alumina invariant line at about 8 wt% alumina is reached. Further additions of alumina will not dissolve, but more bath will solidify to make up for the enthalpy of heating.

The above calculation illustrates the importance of rapid dispersion of the added alumina into a large volume.

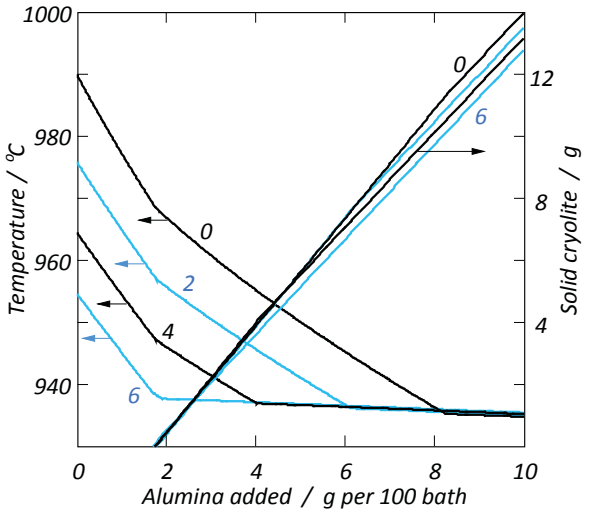

Figure 2. Temperature and amount of solid cryolite formed upon addition of alumina at adiabatic conditions (see text). The initial superheat was 10 °C, and the numbers in the figure refer to the original amount of alumina in the bath (wt%).

Re-melting of Frozen Bath

As already mentioned; when cold alumina hits the bath surface, a layer of frozen bath will form around the particles, and dissolution can not take place until this layer has melted away. From analytic models for the time needed for re-melting, it has been shown [8, 9] that this time is only a small fraction of the total time needed for dissolution. This part of the process is, of course, heat transport controlled.

Dissolution

Alumina does not simply dissolve; it reacts with the bath to form anion complexes such as $Al_2OF_6^{2-}$ and $Al_2O_2F_4^{2-}$ [10]. It has been shown that during the dissolution step, *i.e.*, after establishing direct contact between alumina and bath, the process is mass transfer controlled rather than heat transfer controlled. When the alumina concentration difference between the particle surface and the bulk of the melt is 5 wt%, the corresponding temperature difference due to the heat of dissolution was calculated to be in the range 0.5-2 °C, depending on the geometry of the particle or agglomerate and the flow conditions [11]. There is no information available indicating that the dissolution of alumina in cryolitic melts is not diffusion controlled, provided that the alumina surface is contacting the bath directly.

The Role of Turbulence

It is considered to be an advantage to add alumina to a bath volume that is highly turbulent, which is one of the main reasons for using slotted anodes. Besides causing dispersion of alumina into a large volume and thereby providing enough heat for dissolution, turbulence also enhances the dissolution itself. This is because turbulence prevents the formation of large agglomerates, but also because the agglomerates experience higher shear forces than in a quiescent bath, which enhances the rates of mass- and heat transfer.

Turbulence probably works more effectively on agglomerates than on single alumina grains. Since the length scale of the turbulence (in the order 10^{-2}-10^{-1} m) is so much larger than the dimension of the particles (10^{-5}-10^{-4} m), the turbulence does not lead to shear forces at the particle surface; individual alumina grains just "follow the stream". The turbulence mainly acts by increasing the acceleration necessary for setting up a relative velocity between the particle and the liquid. The initial vortices caused by the gas bubbles can be assumed to have dimensions and velocities comparable to the bubbles, *i.e.*, tangential velocity (v_t) in the order of 10^{-1} ms^{-1} and radius (r) in the order 10^{-2}-10^{-1} m. The acceleration of an alumina grain sitting in such a swirl is comparable with the acceleration of gravity,

$$a = \frac{v_t}{r} = 1-10\,m\,s^{-2} \qquad (1)$$

Dissolution of Single Alumina Particles

In the following, only dissolution of individual alumina particles will be treated. The particles are regarded as spheres. As already mentioned, the re-melting period will be small compared with the dissolution period. The physical data used in the calculations are shown in Table I.

Table I. Physical data used in calculations.

Parameter	Symbol, dimension		Value
Theoretical alumina density	ρ_a	kgm^{-3}	4000
Porosity, alumina particle	φ	1	0.5
Density, bath	ρ	kgm^{-3}	2080
Density, alumina particle *)	ρ_p	kgm^{-3}	3040
Diffusion coefficient, alumina	D	m^2s^{-1}	$1.5 \cdot 10^{-9}$
Kinematic viscosity, bath	ν	m^2s^{-1}	$1.3 \cdot 10^{-6}$

*) Assuming that all pores are filled with bath

Mass Transfer Coefficient

According to Bird *et al.* [12], the mass transfer coefficient at a sphere can be calculated from the following relationship between the dimensionless Sherwood (Sh), Reynolds (Re), and Schmidt (Sc) numbers,

$$Sh = 2 + 0.6\,Re^{\frac{1}{2}} \cdot Sc^{\frac{1}{3}}$$

where (2)

$$Sh = \frac{k\,d}{D}; \quad Re = \frac{u\,d}{\nu}; \quad Sc = \frac{\nu}{D}$$

In this equation, k is the mass transfer coefficient [ms^{-1}], d is the diameter of the sphere [m], D is the diffusion coefficient [m^2s^{-1}], u is the relative velocity between the sphere and the liquid [ms^{-1}], and ν is the kinematic viscosity [m^2s^{-1}]. The constant in Equation (2) is due to the spherical geometry, leading to steady-state mass transfer even when the particle is surrounded by a quiescent fluid.

Dissolution without Relative Motion

If the alumina particles are very small, or if they do not move through the bath, the last term in Equation (2) will be negligible. In this case, the mass transfer coefficient becomes

$$k = \frac{2D}{d} \tag{3}$$

and it was shown [11] that the time of dissolution (t_d) can be calculated analytically by

$$t_d = \frac{d^2 \rho_a (1-\varphi)}{8D(w_* - w_b)\rho} \tag{4}$$

where w_* and w_b are the weight fractions of alumina at the particle surface and in the bulk, respectively, and the other symbols are explained in Table I. By inserting data from Table I, we obtain

$$t_d = \frac{8.01 \cdot 10^7 \cdot d^2}{w_* - w_b} \tag{5}$$

which gives a dissolution time of 12.8 s for a 80 µm grain when the concentration difference between surface and bulk is 4 weight percent. Equation (4) represents the maximum time for dissolution, since the convectional contribution was neglected.

Dissolution of Particles Falling through Quiescent Bath

If the particle's motion through the bath is taken into consideration the time for dissolution will be shorter, especially for the larger grains. We assume that the relative velocity between particle and liquid corresponds to the terminal velocity of the particle when subjected to graviational forces in quiescent bath, although turbulence may add to the acceleration of gravity (Equation (1)).

Figure 3 shows the results from a numerical calculation using standard equations for the drag between a sphere and a liquid [12]. The resulting terminal velocity was used in Equation (2) to calculate the diameter of the shrinking particle as a function of time. As can be observed, the rate of shrinkage increases as the particle becomes smaller; this is because the mass transfer coefficient becomes very large at the surface of small spheres (Equation (2)).

The bath height is normally about 20 cm in an industrial cell. By comparing the time for dissolution and the terminal velocity in Figure 3, it can easily be found that even the biggest alumina grains will dissolve before they reach the metal, unless the bath is close to alumina saturation. Independent of the mass transfer conditions, the time for dissolution will be inversely proportional with the difference beween saturation and the actual concentration.

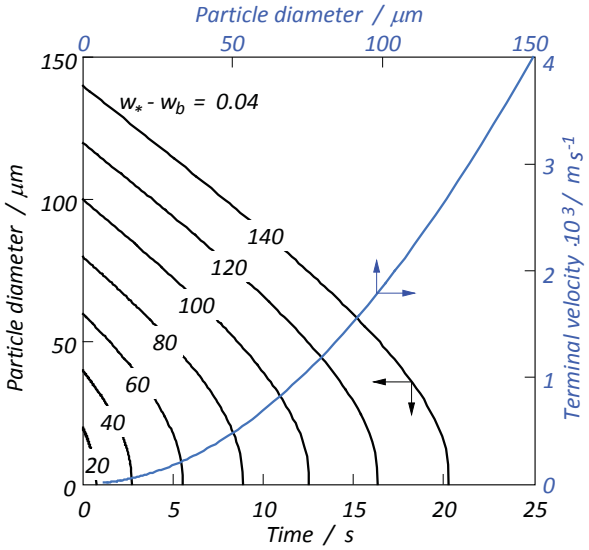

Figure 3. Alumina particle diameter as a function of time during dissolution (left hand scale) and terminal velocity as a function of the particle diameter (right hand scale). The numbers in the figure refer to the initial diameter of the alumina grain. The alumina concentration difference between the particle surface and the bulk was taken to be 4 weight percent.

Amount of Alumina Dispersed in the Bath

The theoretical consumption rate of alumina in a 300 kA cell running at 94 percent current efficiency equals 4293 kg/day or 49.7 g/s. If the alumina concentration in the electrolyte is constant, the consumption rate and the dissolution rate are exactly balanced. It may be interesting to look into how much alumina must be dispersed in the bath in order to keep up with the consumption.

As a simplification, we first assume that the alumina particles all have the same initial diameter (d_0). The average rate of dissolution of N grains becomes

$$J_d = N \cdot \frac{\frac{\pi}{6} d_0^3 \rho_a (1-\varphi)}{t_d} \qquad [kgs^{-1}] \tag{6}$$

Furthermore, the time-averaged mass of an alumina particle (m_{av}) during dissolution can be calculated by

$$m_{av} = \frac{m_0}{t_d} \int_0^{t_d} \left(\frac{d}{d_0} \right)^3 dt \tag{7}$$

where the subscript "0" refers to the initial dimensions. In the case of very small particles or when there is zero relative velocity between particle and liquid (when Equation (4) is valid), it can readily be found analytically that $m_{av}/m_0 = 2/5$. For larger alumina grains, this number decreases slightly; *e.g.*, for 80 μm particles, $m_{av}/m_0 \approx 0.36$. The time of dissolution can be calculated numerically as shown in Figure 3. Therefore, we have enough information to estimate the necessary amount of dispersed alumina in the bath, since Equation (6) gives the number of particles and Equation (7) gives the average mass of each particle.

The mass of dispersed alumina needed to maintain electrolysis in a 300 kA cell at different alumina concentrations and different particle sizes is shown in Figure 4. It is astonishing and thought-provoking that a few hundred grams of dispersed alumina suffices to keep a 300 kA cell running. Indeed, this estimate was the real starting point of the present paper.

In reality, the alumina will contain a wide range of grain sizes, but this does not really change the conclusion in the above simplified calculation. The smallest alumina grains disappear almost immediately after feeding, while larger grains remain in the bath for a longer time. The average diameter decreases, however, because the particles shrink during dissolution (Equation (7)). Together, these two effects bring about a somewhat smaller average diameter and narrower particle size distribution in the bath than in the feed.

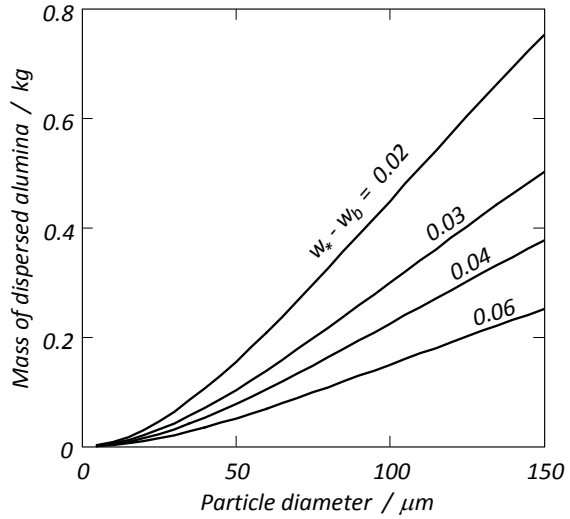

Figure 4. Necessary mass of dispersed alumina in a 300 kA cell running at 94 percent current efficiency as a function of the alumina grain diameter. The concentration differences between the particle surface and the bulk are given in the figure.

Conditions for Dispersion of Alumina as Single Grains

As would be evident from the above estimates; the dissolution of alumina will not represent a problem when the feed really is dispersed as single grains. It is already known that part of the alumina end up as free particles. Kobbeltvedt *et al.* [13] added batches of 0.45 g/alumina per cm^2 bath surface in a laboratory cell, and it was found that part of the added amount dissolved within a few seconds. The fraction of the batch that dissolved immediately could be increased by preheating, gas bubbling, and mechanical stirring. It was also observed that secondary alumina dissolved more rapidly than virgin alumina, which was related to higher contents of volatiles in the secondary alumina, giving more intense stirring at the surface.

The above observations demonstrate that stirring at the bath surface is important. When adding relatively large batches, stirring and preheating apparently work by preventing sintering of alumina particles stacked at the bath surface.

To allow all the alumina to dissolve as individual grains, it seems necessary to apply slower feeding, *i.e.*, using smaller batches. The necessary conditions for avoiding formation of agglomerates are derived below.

Basic Assumptions

A very simple model for estimates concerning agglomeration or not can be derived under the following conditions,

- During the feeding period, the alumina is spread uniformly in time and space to a surface area A [m^2].
- Feeding takes place in a dimensionless time span τ_{feed} defined as the ratio between the feeding time and the total time (*e.g.*, $\tau_{feed} = 3/60 = 0.05$ if the alumina is trickled onto the bath surface in a steady stream for 3 seconds every 60 seconds).
- All alumina particles have the same diameter.
- A short distance below the bath surface, the alumina particles move downwards with their initial terminal velocity u_T.
- The total consumption of alumina in the cell is J_{el} [kgs^{-1}], *e.g*, $J_{el} = 0.05$ kgs^{-1} in a 300 kA cell.

Criterion Based on Volume Fraction of Alumina

An obvious condition for achieving agglomeration-free alumina feeding is that the volume fraction of alumina at and close to the bath surface is far below unity, also during feeding, to reduce the risk of particles contacting each other and freezing together.

At quasi-stationary conditions, the consumption rate of alumina equals the time-averaged feeding rate,

$$J_{el} = A \cdot \tau_{feed} \cdot c \cdot u_T \qquad [kgs^{-1}] \tag{8}$$

where c is the concentration of alumina in the form of particles [kgm^{-3}]. Turbulence near the surface will contribute in spreading the alumina (increase the area). Still, the terminal velocity in quiescent bath is used in Equation (8), since the vertical component of the convection is small close to the surface.

The concentration of solid alumina is related to the volume fraction of alumina particles (ψ) and the particle alumina density,

$$c = \psi \cdot \rho_a (1-\varphi) \quad [kgm^{-2}s^{-1}] \tag{9}$$

Agglomeration will not happen if there are large distances between the alumina particles, *i.e.*, when $\psi << 1$. The criterion for dispersion as individual grains can then be found by combination of Eqs. (8) and (9),

$$\psi = \frac{J_{el}}{A \cdot \tau_m \rho_a (1-\varphi) \cdot u_T} << 1 \tag{10}$$

We may now check if today's point feeders fulfil this criterion. As an example, we assume a consumption rate J_{el} = 0.05 kgs^{-1} (300 kA cell), feeding area A = 0.28 m^2 (*e.g.*, 4 feeders supplying alumina to areas each 30 cm in diameter), dimensionless feeding time τ_{feed} = 0.05 (3 s feeding each 60 s), particle alumina density $\rho_a(1 - \varphi)$ = 2000 kgm^{-3}, and terminal velocity u_T = 0.0012 ms^{-1} (80 μm particle). These numbers give a particle volume fraction ψ = 1.49, which is clearly too high to fulfil the criterion in Equation (10). However, by increasing the dimensionless feeding time to 0.8 (almost continuous feeding) the volume fraction decreases to 0.09, which is probably low enough to avoid agglomeration.

Criterion Based on Risk of Collision

As an alternative, it is possible to derive the criterion for agglomeration or dispersion as individual particles by evaluating the risk of collision between an alumina particle that has just landed on the bath surface and a succeeding particle. As above, we assume that the alumina particles are equally sized.

The number of particles landing at the bath surface per second and unit area during feeding becomes

$$\dot{N} = \frac{J_{el}}{A \cdot \tau_m \cdot \frac{\pi}{6} \cdot d^3 \cdot \rho_a (1-\varphi)} \qquad [s^{-1}m^{-2}] \qquad (11)$$

A particle falling through the air and hitting the bath will penetrate the surface and then decelerate to its terminal velocity. Figure 5 shows the calculated position as a function of time for alumina particles hitting the bath with a velocity of 2 ms^{-1} (corresponds to a free fall of 0.2 m). Splashing was not taken into consideration. The figure illustrates that it may be a good approximation to assume that the particles have "air velocity" down to a certain position (*e.g.*, 0.29 mm from the surface for a 100 μm particle) and "bath velocity" u_T from then on.

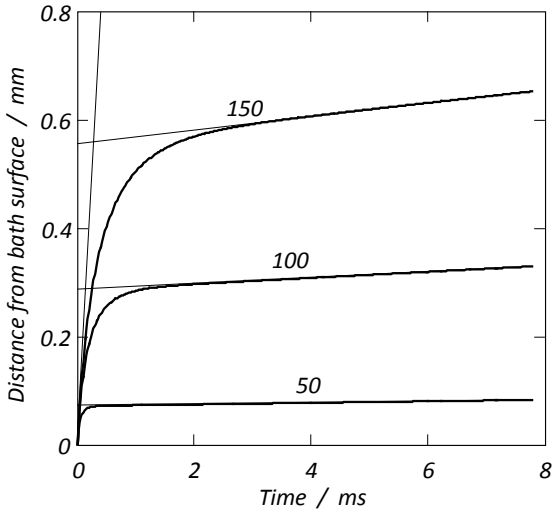

Figure 5. Position as a function of time for alumina particles with different diameters (μm, given in the figure) hitting the bath surface with a velocity of 2 ms^{-1}. The dotted lines represent the initial velocity and the terminal velocity through the bath.

Once the particle has slowed down to its terminal velocity, it will be available for collision with a succeeding particle until it has moved one particle diameter further down, as illustrated in Figure 6 a). This corresponds to a time d/u_T. Provided equal particle diameters, the collision diameter is twice the particle diameter (Figure 6 b)).

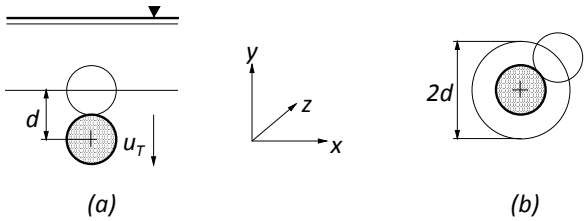

Figure 6. a) – the particle will be available for collision with a succeeding particle down to a distance of one particle diameter from the plane where the terminal velocity is reached, b) – the collision diameter is twice the particle diameter.

A particle that is available for collision covers a (maximum) surface area in the xz plane

$$\alpha = \pi d^2 \quad [m^2] \qquad (12)$$

The number of alumina particles landing within this collision area per unit of time becomes

$$\dot{n} = \dot{N} \cdot \alpha = \frac{6 J_{el}}{A \cdot \tau_m \cdot d \cdot \rho_a (1-\varphi)} \qquad [s^{-1}] \qquad (13)$$

and a particle being available for collision for d/u_T s will be hit n_{hit} times,

$$n_{hit} = \dot{n} \cdot \frac{d}{u_T} \qquad (14)$$

It is reasonable to assume that each alumina particle in average must collide less than once to avoid agglomeration. This gives the criterion

$$n_{hit} = \frac{6 J_{el}}{A \cdot \tau_m \cdot \rho_a (1-\varphi) \cdot u_T} < 1 \qquad (15)$$

and this turns out to be basically the same expression as Equation (10) above.

By using the same data as in the preceding section we obtain n_{hit} = 8.9 with today's point feeders, which clearly must lead to agglomeration. Increasing the dimensionless feeding time to 0.8 gives n_{hit} = 0.56, which may be acceptable.

Discussion

Alumina Grains with Different Sizes

All calculations in the present work were made assuming alumina particles with uniform diameter. From Figure 5 it can be observed that smaller grains travel a shorter distance in the bath before they attain their terminal velocity, and the terminal velocity is also smaller than for larger particles. This means that small grains risk being caught up and hit by larger succeeding grain, but on the other hand; a large grain will never collide with a smaller succeeding grain. It is difficult to predict how this influences the

critical feeding rate when agglomeration starts. As a thought experiment, we may imagine that the alumina contains two classes of particle size with equal number of members in each. Even when each and every small grain is caught up by a large grain, agglomeration will still be avoided if only a small fraction of the large grains collide.

Particles with Frozen Bath

When cold alumina hits the bath, a coat of frozen bath is formed immediately. The heat needed for transformation of 1 kg γ-Al_2O_3 at 25 ^oC to α-Al_2O_3 at 960 ^oC is 870 kJ, while the heat of melting of bath is about 512 kJ/kg. This means that one kg alumina freezes out 1.7 kg bath. If the freeze coat is formed instantaneously, the maximum diameter of the alumina particle with freeze becomes 29 percent larger than the original particle, given a density of 2900 kgm^{-3} for the frozen bath.

The diameter, density, and terminal velocity for a typical alumina particle with or without freeze are shown in Table II. It is not known to which degree bath will penetrate into the particle during freezing, so the density and terminal velocity were calculated for the two extreme alternatives. In all cases, the terminal velocities are well within the same order of magnitude.

Although the calculations in the present paper are simplistic, it is believed that the derived criterion, Equation (10) or Equation (15), provides a realistic first estimate.

Table II. Diameter, density, and terminal velocity in bath for a typical alumina particle with or without frozen bath.

	Diameter μm	Density kgm^{-3}	Velocity mms^{-1}
Without freeze, air inside	80	2000	-
Without freeze, bath inside	80	3040	1.20
With freeze, air inside	104	2486	0.85
With freeze, bath inside	104	2964	1.83

Possibilities of Realising a Non-Agglomerate Alumina Feeder

Some patents have been filed concerning devices for continuous alumina feeding. The inventions comprise trickling of alumina by means of dual flow passages [14], a vertical feeding tube supplied with a variable valve [15], an inert anode with an alumina feeding duct integrated in the anode stem [16], and a horizontal tube for blowing the alumina into the gap between the bath and the crust [17]. Furthermore, it has been proposed [18] to feed the alumina through a narrow slot placed above the bath, and recently, a modified feeder tube leading to longer time for addition of alumina was demonstrated [19].

To the author's knowledge, continuous feeding has not yet been introduced commercially. While the suggested devices may work properly in the laboratory, fluoride vapour and splashing of bath in industrial cells will cause problems related to clogging as well as to materials stability. Those issues may be possible to resolve, however.

Acknowledgement

The present work was mainly financed by Hydro. Permission to publish the results is gratefully acknowledged.

References

1. R. Ødegård, S. Rønning, S. Rolseth, and J. Thonstad, "On Alumina Phase Transformations and Crust Formation in Aluminum Cells", Light Metals 1985, pp. 695/709.
2. G.P. Tarcy, H. Kvande, and A. Tabereaux, "Advancing the Industrial Aluminum Process: 20th Century Breakthrough Inventions and Developments", *Journal of Metals*, **63** (8), pp. 101/08 (2011).
3. O. Martin, S. Despinasse, C. Ritter, R. Santerre, and T. Tomasino, "The FECRI Approach and the Latest Developments in the AP3X Technology", Light Metals 2008, pp. 255/60.
4. M.W. Chase *et al*. (Ed.), *J. Phys. Ref. Data*, Vol. 14, Suppl. 1, 1985 (JANAF Thermochemical Data).
5. A. Solheim and Å. Sterten, "Activity of Alumina in the System NaF-AlF_3-Al_2O_3 at NaF/AlF_3 Molar Ratios Ranging from 1.4 to 3", Light Metals 1999, pp. 445/52.
6. A. Solheim, S. Rolseth, E. Skybakmoen, L. Støen, Å. Sterten, and T. Støre, Liquidus Temperatures for Primary Crystallization of Cryolite in Molten Salt Systems of Interest for the Aluminium Electrolysis", *Met. Trans. B* **27B** (1996), pp. 739/44.
7. E. Skybakmoen, A. Solheim, and Å. Sterten, "Alumina Solubility in Molten Salt Systems of Interest for Aluminium Electrolysis and Related Phase Diagram Data", *Met. Trans. B* **28B** (1997), pp. 81/86.
8. O.A. Asbjørnsen and J.A. Andersen, "Kinetics and Transport Processes in the Dissolution of Aluminium Oxide in Cryolite Melts, Light Metals 1977, Vol. 1, pp. 137/52.
9. R. Hovland, R. Rolseth and A. Solheim, "On the Alumina Dissolution in Cryolitic Melts", Proceedings of the International Symposium on Light Metals Processing and Applications, Quebec City, August 29-September 1, 1993, pp. 3/16.
10. J. Thonstad, P. Fellner, G.M. Haarberg, J. Hives, H. Kvande, and Å. Sterten, Aluminium Electrolysis, 3rd Edition, Aluminium-Verlag, Düsseldorf, 2001, pp. 76/8.
11. J. Thonstad, A. Solheim, S. Rolseth, and O. Skar, "The Dissolution of Alumina in Cryolite Melts", Light Metals 1988, pp. 655/61.
12. R.B. Bird, W.E. Stewart, and E.N. Lightfoot, Transport Phenomena, p. 333, John Wiley & Sons, Inc., New York, 1960.
13. O. Kobbeltvedt, S. Rolseth, and J. Thonstad, "On the Mechanisms of Alumina Dissolution with Relevance to Point Feeding Aluminium Cells", Light Metals 1996, pp. 421/27.
14. B.J. Welch *et al*., "Trickle Alumina Feeder", WO/1993/14248.
15. B.J. Welch *et al*., "Continuous Alumina Feeder", WO/1993/14247.
16. G. Berclaz and V. de Nora, "Electrolytic Cell with Improved Feed Device", WO/2006/129267.
17. T.T. Nguyen and V. de Nora, "Electrolytic Cell with Improved Feed Device", WO/2004/050957.
18. A.I. Begunov and Ye.V. Kudryavtseva, "A Device for Continuous Alumina Feed to Aluminium Reduction Cells", Light Metals 1997, pp. 211/14.
19. J. Tessier, G.P. Tarcy, E. Batista, X. Wang, and P. Doiron, "Improvement of Alumina Dissolution Rate through Alumina Feeder Pipe Modification", Light Metals 2013, pp. 713/18.